Cell Reports

Article

The Zscan4-Tet2 Transcription Nexus Regulates Metabolic Rewiring and Enhances Proteostasis to Promote Reprogramming

Graphical Abstract

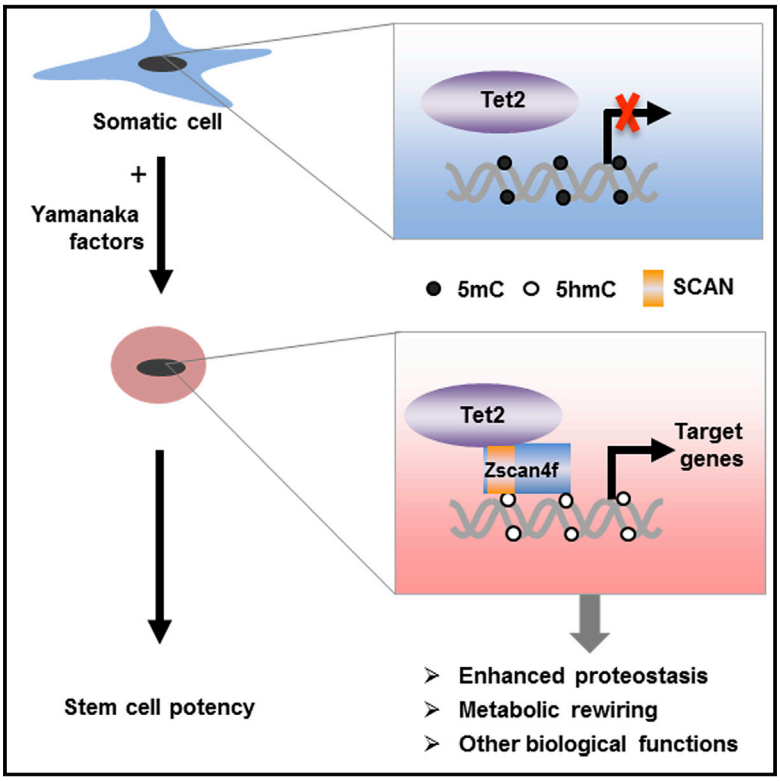

Highlights

- Zscan4f is a sequence-specific DNA-binding transcription factor
- Zscan4f, a representative of ZSCAN proteins, is a functional partner for Tet2
- The ZSCAN4-TET2 complex regulates metabolic rewiring and activates proteasome activity
- Recruiting TET may represent a general biochemical mechanism of ZSCAN proteins

Authors

Zhou-Li Cheng, Meng-Li Zhang, Huai-Peng Lin, ..., Yue Xiong, Mingliang Zhang, Dan Ye

Correspondence

mingliang.zhang@shsmu.edu.cn (M.Z.), yedan@fudan.edu.cn (D.Y.)

In Brief

Cheng et al. show that Zscan4f recruits Tet2 to target gene promoters, promotes DNA demethylation, regulates metabolic rewiring, and activates proteasome activity, indicating a mechanism of Zscan4 to control cell fate. This study also uncovers a potential and common biochemical mechanism shared by the SCAN family to recruit TET enzymes.

Cheng et al., 2020, Cell Reports *32*, 107877
July 14, 2020
https://doi.org/10.1016/j.celrep.2020.107877

CellPress

Cell Reports

CellPress
OPEN ACCESS

Article

The Zscan4-Tet2 Transcription Nexus Regulates Metabolic Rewiring and Enhances Proteostasis to Promote Reprogramming

Zhou-Li Cheng,[1,2] Meng-Li Zhang,[1,3] Huai-Peng Lin,[4] Chao Gao,[1,2] Jun-Bin Song,[1,2] Zhihong Zheng,[5] Linpeng Li,[6] Yanan Zhang,[7] Xiaoqi Shen,[7] Hao Zhang,[8] Zhenghui Huang,[9] Wuqiang Zhan,[1,2] Cheng Zhang,[1,2] Xu Hu,[10] Yi-Ping Sun,[1,2] Lubing Jiang,[9] Lei Sun,[1,2] Yanhui Xu,[1,2] Chen Yang,[8] Yuanlong Ge,[11] Yong Zhao,[11] Xingguo Liu,[6] Hui Yang,[3] Pengyuan Liu,[12] Xing Guo,[7] Kun-Liang Guan,[13] Yue Xiong,[14] Mingliang Zhang,[10,*] and Dan Ye[1,2,15,16,*]

[1]Huashan Hospital, Fudan University, and Molecular and Cell Biology Lab, the Shanghai Key Laboratory of Medical Epigenetics, Institutes of Biomedical Sciences, Fudan University, and the Key Laboratory of Metabolism and Molecular, Ministry of Education, Shanghai, China

[2]The International Co-laboratory of Medical Epigenetics and Metabolism, Ministry of Science and Technology, Beijing, China

[3]Department of Neurosurgery, Huashan Hospital, Fudan University, Shanghai 200040, China

[4]Medical College of Xiamen University, Xiamen 361102, China

[5]Department of Gynecologic Oncology, Women's Hospital and Institute of Translational Medicine, School of Medicine, Zhejiang University, Hangzhou, Zhejiang 310029, China

[6]The Key Laboratory of Regenerative Biology, Guangdong Provincial Key Laboratory of Stem Cell and Regenerative Medicine, South China Institute for Stem Cell Biology and Regenerative Medicine, Guangzhou Institutes of Biomedicine and Health, Chinese Academy of Sciences, Guangzhou 510530, China

[7]Life Sciences Institute, Zhejiang University, Hangzhou 310058, China

[8]Key Laboratory of Synthetic Biology, Institute of Plant Physiology and Ecology, Shanghai Institutes for Biological Sciences, Chinese Academy of Sciences, Shanghai 200032, China

[9]Institute Pasteur of Shanghai, Chinese Academy of Sciences, Shanghai 200031, China

[10]Department of Histoembryology, Genetics and Developmental Biology, Shanghai Jiao Tong University School of Medicine, Shanghai Key Laboratory of Reproductive Medicine, Shanghai, China

[11]MOE Key Laboratory of Gene Function and Regulation, State Key Laboratory of Biocontrol, School of Life Sciences, Sun Yat-sen University, Guangzhou 510006, China

[12]Department of Respiratory Medicine, Sir Run Run Shaw Hospital and Institute of Translational Medicine, School of Medicine, Zhejiang University, Hangzhou, Zhejiang 310016, China

[13]Department of Pharmacology and Moores Cancer Center, University of California San Diego, La Jolla, CA 92093, USA

[14]Department of Biochemistry and Biophysics, Lineberger Comprehensive Cancer Center, University of North Carolina at Chapel Hill, Chapel Hill, NC 27599, USA

[15]Department of General Surgery, Huashan Hospital, Fudan University, Shanghai 200040, China

[16]Lead Contact

*Correspondence: mingliang.zhang@shsmu.edu.cn (M.Z.), yedan@fudan.edu.cn (D.Y.)

https://doi.org/10.1016/j.celrep.2020.107877

SUMMARY

Evolutionarily conserved SCAN (named after SRE-ZBP, CTfin51, AW-1, and Number 18 cDNA)-domain-containing zinc finger transcription factors (ZSCAN) have been found in both mouse and human genomes. Zscan4 is transiently expressed during zygotic genome activation (ZGA) in preimplantation embryos and induced pluripotent stem cell (iPSC) reprogramming. However, little is known about the mechanism of Zscan4 underlying these processes of cell fate control. Here, we show that Zscan4f, a representative of ZSCAN proteins, is able to recruit Tet2 through its SCAN domain. The Zscan4f-Tet2 interaction promotes DNA demethylation and regulates the expression of target genes, particularly those encoding glycolytic enzymes and proteasome subunits. Zscan4f regulates metabolic rewiring, enhances proteasome function, and ultimately promotes iPSC generation. These results identify Zscan4f as an important partner of Tet2 in regulating target genes and promoting iPSC generation and suggest a possible and common mechanism shared by SCAN family transcription factors to recruit ten-eleven translocation (TET) DNA dioxygenases to regulate diverse cellular processes, including reprogramming.

INTRODUCTION

The ten-eleven translocation (TET) family of proteins catalyze three sequential oxidation reactions: first converting 5-methylcytosine (5mC) to 5-hydroxymethylcytosine (5hmC), then to 5-formylcytosine (5fC), and finally to 5-carboxylcytosine (5caC), leading to eventual DNA demethylation (He et al., 2011; Ito et al., 2011; Kohli and Zhang, 2013). All three TET proteins contain a

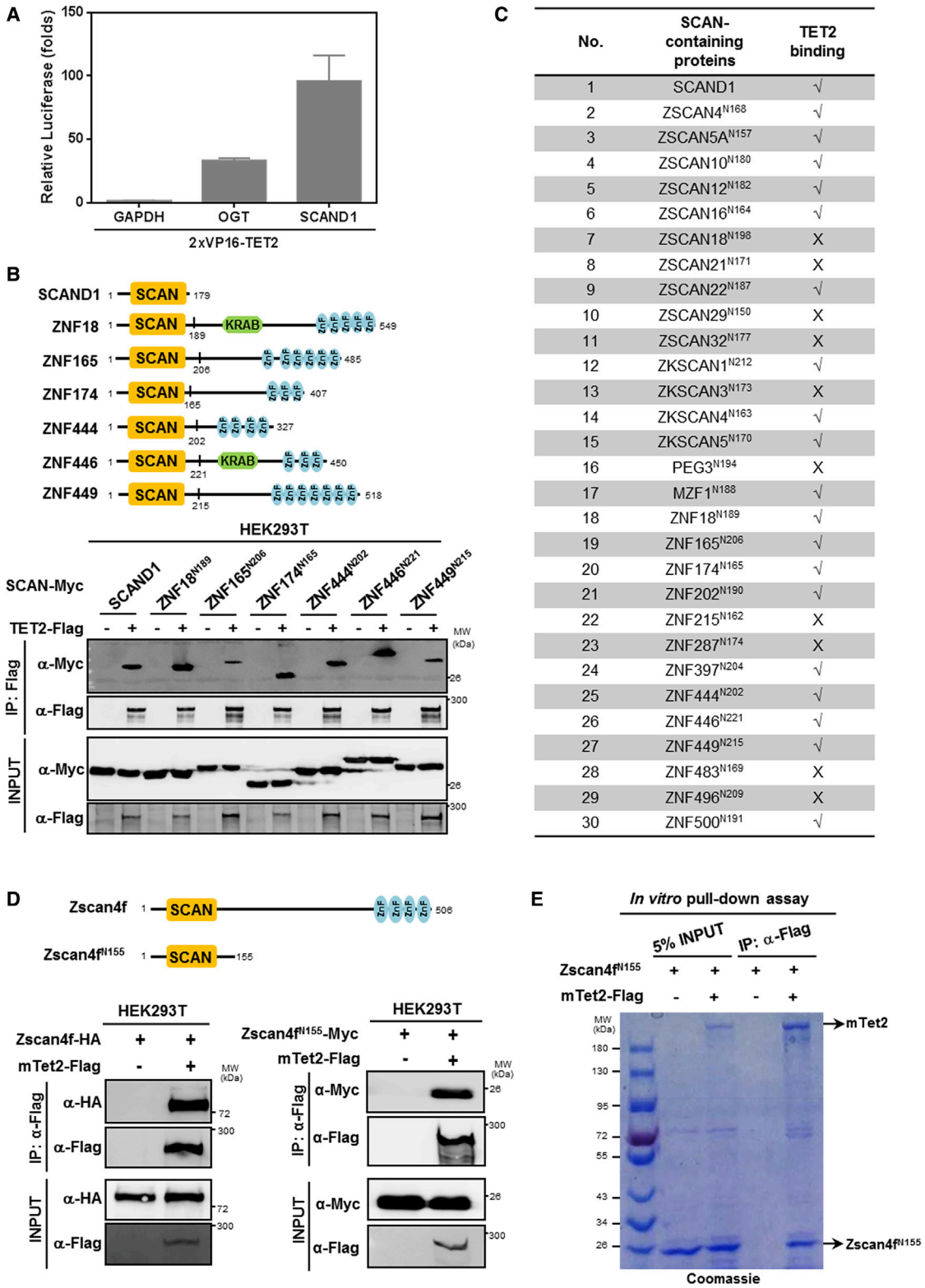

No.	SCAN-containing proteins	TET2 binding
1	SCAND1	√
2	ZSCAN4^{N168}	√
3	ZSCAN5A^{N157}	√
4	ZSCAN10^{N180}	√
5	ZSCAN12^{N182}	√
6	ZSCAN16^{N164}	√
7	ZSCAN18^{N198}	X
8	ZSCAN21^{N171}	X
9	ZSCAN22^{N187}	√
10	ZSCAN29^{N150}	X
11	ZSCAN32^{N177}	X
12	ZKSCAN1^{N212}	√
13	ZKSCAN3^{N173}	X
14	ZKSCAN4^{N163}	√
15	ZKSCAN5^{N170}	√
16	PEG3^{N194}	X
17	MZF1^{N188}	√
18	ZNF18^{N189}	√
19	ZNF165^{N206}	√
20	ZNF174^{N165}	√
21	ZNF202^{N190}	√
22	ZNF215^{N162}	X
23	ZNF287^{N174}	X
24	ZNF397^{N204}	√
25	ZNF444^{N202}	√
26	ZNF446^{N221}	√
27	ZNF449^{N215}	√
28	ZNF483^{N169}	X
29	ZNF496^{N209}	X
30	ZNF500^{N191}	√

Figure 1. TET2 Physically Interacts with Multiple SCAN Domain Proteins

(A) A mammalian two-hybrid system and dual-luciferase reporter system to search for TET2-interacting proteins. Human full-length (FL) TET2 fused to VP16 transactivation domain (AD), preys fused to Gal4 DNA-binding domain (DBD), UAS-luciferase reporter plasmid, and CMV-Renilla control plasmid were

(legend continued on next page)

conserved and cysteine-rich dioxygenase (CD) domain in their C-terminal region that binds to Fe(II) and α-ketoglutarate (α-KG) to catalyze the oxidation reaction (Iyer et al., 2009; Tahiliani et al., 2009). The N-terminal region of three TET proteins is more divergent and uncharacterized so far, except for a CXXC-type zinc finger (ZF-CXXC) at the N terminus of TET1 and TET3, which selectively recognizes an unmodified CpG dinucleotide (Ko et al., 2013). However, TET2 lacks the ZF-CXXC DNA-binding domain and instead interacts with the neighboring IDAX (inhibition of the Dvl and axin complex protein, also known as CXXC4) (Ko et al., 2013). Although all Tet family members possess 5mC oxidation activity, they show a distinct expression pattern and may exert nonredundant biological functions in different cell types and tissues (Ito et al., 2010).

How Tet proteins achieve diverse functions is not yet well understood, and the specificity could be regulated by their interacting partners, particularly transcription factors (TFs) that recognize specific DNA sequences to control chromatin status and transcription. Supporting this notion, several TFs interacting with Tet have been described, including PU.1, WT1, Nanog, Sall4, and Zfp281 (Costa et al., 2013; de la Rica et al., 2013; Fidalgo et al., 2016; Wang et al., 2015; Xiong et al., 2016). In addition, the RNA-binding protein PSPC1 also recruits TET2 and catalyzes 5hmC modification of MERVL RNAs, resulting in their destabilization and transcriptional repression (Guallar et al., 2018). Of three Tet enzymes, Tet2 is the family member most important for somatic cell reprogramming, as evidenced by the finding that knockdown of *Tet2* totally abrogates the induced pluripotent stem cell (iPSC) colony formation in mouse embryonic fibroblast cells (Doege et al., 2012). Moreover, Tet2 interacts with and is recruited by C/EBPα, Klf4, or Tfcp2l1 to specific genome loci, such as enhancers and promoters of key pluripotency factors, which become demethylated as early as 1 day after Yamanaka factor induction (Sardina et al., 2018). To gain a more comprehensive view on the TET2-TF interaction, we have previously carried out a mammalian two-hybrid screen of a human TF library containing 1,126 known or putative DNA-binding proteins (Zhao et al., 2008) and identified multiple transcriptional regulators that potentially interact with TET2 (Chen et al., 2018). These findings provide evidence to support a general mechanism underlying TET2 targeting to particular genes through interacting with a DNA-sequence-specific TF. Among the positive TET2 interactions is SCAN (named after SRE-ZBP, CTfin51, AW-1, and Number 18 cDNA) domain containing 1 (SCAND1), which contains an isolated and highly conserved motif of approximately 80 amino acids, known as the SCAN domain (Williams et al., 1995). The SCAN domain was evolved from the gag protein of Gypsy/Ty3-like retrotransposons in limbed vertebrates (Emerson and Thomas, 2011) and is found near the N terminus of a subfamily of Cys_2-His_2 (C_2H_2) SCAN-domain-containing zinc finger TFs (ZSCAN) (Edelstein and Collins, 2005). Further study of SCAND1-TET2 interaction led to the discovery of a mechanism for guiding Tet2 to specific DNA regions in the genome through interaction with Zscan4f, a member of ZSCAN.

RESULTS

TET2 Interacts with Multiple SCAN Family TFs

How TET2, like other chromatin-modifying enzymes that in general do not have specific DNA-binding domains, is recruited to specific sites in the genome to regulated target genes is not fully understood. By using TET2 as bait, we carried out a mammalian two-hybrid screen of a human TF library to comprehensively identify DNA-binding proteins that potentially interact with TET2 in HEK293T cells. Among the positive interactions, SCAND1 exhibited strong luciferase reporter activation (Figure 1A). We then confirmed SCAND1-TET2 interaction by co-immunoprecipitation (co-IP) and western blot (Figure 1B). SCAND1 is a SCAN-domain-only protein without a zinc finger motif, implying that the SCAN domain may interact with TET2.

Human and mouse genomes encode 57 and 43 ZSCAN proteins, respectively (Figures S1A and S1B), accounting for nearly 10% of the C_2H_2 zinc finger genes. To explore whether the SCAN domain contributes to the interaction with TET2, we cloned the SCAN-box from 30 human *ZSCAN* genes and observed that 20 of them interacted with TET2 when co-overexpressed in HEK293T cells (Figures 1B, 1C, and S1C). We further demonstrated that these SCAN proteins, including ZSCAN4, could interact with endogenous TET2 in human breast cancer MCF7 cells and bone osteosarcoma U2OS cells (Figure S1D). Unlike the human genome that expresses only one ZSCAN4, mouse Zscan4 locus contains 6 paralogs and 3 pseudogenes (Falco et al., 2007). Among them, Zscan4a, Zscan4b, and Zscan4e lack the DNA-binding C_2H_2 zinc finger domain, whereas Zscan4c, Zscan4d, and Zscan4f contain both the SCAN-box and zinc finger domain. When they are co-expressed in HEK293T cells, we found that Tet2 interacted with Zscan4f through its N-terminal 155 residues (referred to as Zscan4f^{N155}), a region only covering the highly conserved SCAN domain

co-transfected in HEK293T cells. At 30 h after transfection, the luciferase reporter activity was measured as an indicator for protein-protein interaction. Gal4(DBD)-tagged GAPDH and O-linked N-acetylglucosamine (GlcNAc) transferase (OGT) were included as a negative and positive control, respectively. Shown are average values of triplicated results with standard error of the mean (SEM).

(B) Structural features of indicated human ZSCAN proteins (top). The conserved domains are shown with shaded boxes: SCAN domain (yellow), KARB domain (green), and C_2H_2 zinc finger domain (blue). FLAG-TET2 was transiently co-expressed with each of Myc-tagged SCAN domains in HEK293T cells. The protein-protein interaction was examined by immunoprecipitation (IP)-western using indicated antibodies.

(C) A summary of tested SCAN-TET2 interaction when co-expressed in HEK293T cells, as described in (B).

(D) Structural features of mouse Zscan4f and truncated proteins (top). FLAG-Tet2 was transiently co-expressed with HA-Zscan4f or the Myc-tagged SCAN domain of Zscan4f (N-terminal 155 residues, referred to as Zscan4f^{N155}) in HEK293T cells. The [rotein-protein interaction was examined by IP-western using indicated antibodies.

(E) *In vitro* pull-down assay shows Zscan4f^{N155} interacts with Tet2 directly. FLAG-Tet2 was ectopically expressed in HEK293T cells and purified by IP with FLAG beads and subsequent FLAG peptide competition. Meanwhile, His-tagged Zscan4f^{N155} was expressed in *Escherichia coli* and purified by IP. These purified proteins were incubated and then immunoprecipitated with FLAG beads to detect Zscan4f^{N155} by Coomassie blue staining.

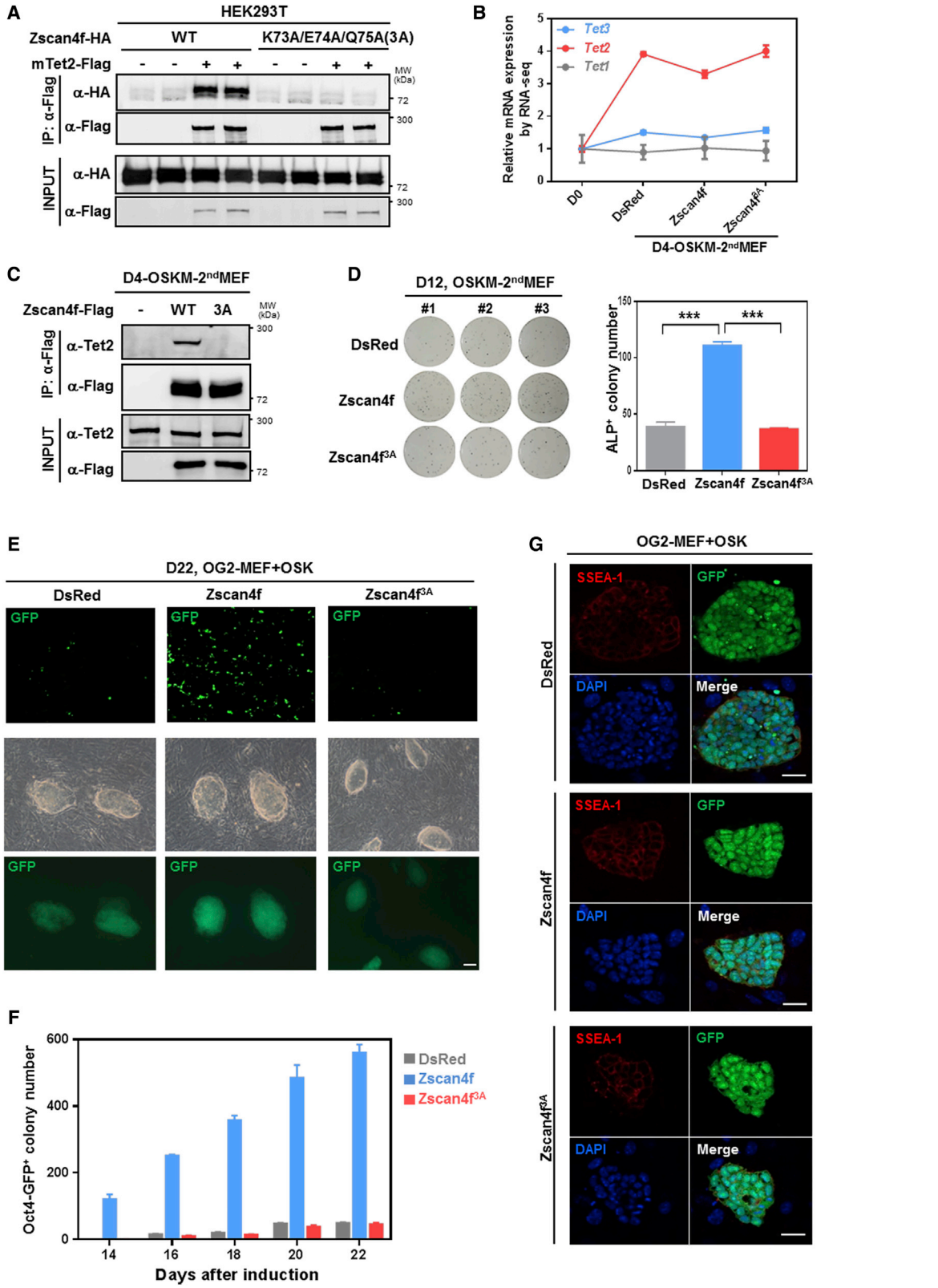

(legend on next page)

(Figure 1D). *In vitro* pull-down assay confirmed that Zscan4f^{N155} directly interacted with Tet2 (Figure 1E).

According to the sequence alignments of mouse SCAN family members, the SCAN domain contains five amphipathic α helices, of which helixes 2 and 3 are the most conserved (Figure S2A). To identify residues in the SCAN-box for Tet2 binding, we focused on the conserved regions while excluding the residues involved in SCAN dimerization, as previously identified by nuclear magnetic resonance (NMR) spectroscopy (Peterson et al., 2006), and carried out a systematic mutagenesis screen to map residues that are important for Tet2 binding. Eventually, we identified that individual mutations of three residues (K73, E74, and Q75) in the SCAN-box of Zscan4f to alanine (A) could partially reduce the association with Tet2 when co-overexpressed in HEK293T cells (Figures S2B and S2C). Importantly, a combined triple mutation (K73A/E74A/Q75A, hereafter referred to as Zscan4f^{3A}) completely eliminated the Zscan4f-Tet2 interaction (Figure 2A). So far, very little is known about the biochemical functions of the SCAN domain, except its role in mediating homo- and heterodimerization (Nam et al., 2004). We found Zscan4f-HA and Zscan4f-green fluorescence protein (GFP) indeed interacted with each other and that triple mutations of K73A, E74A, and Q75A in Zscan4f did not affect Zscan4f dimerization (Figure S2D).

Together, these results demonstrate that Tet2 interacts with many SCAN-containing TFs, including Zscan4f, and that the ZSCAN-TET2 interaction is conserved across species.

Tet2 Interaction Is Important for Zscan4f to Promote iPSC Generation

Both Zscan4 and Tet2 are functionally required for reprogramming fibroblasts to pluripotency (Doege et al., 2012; Hirata et al., 2012). However, whether or not they work synergistically for reprogramming has not been investigated yet. The SCAN domains in Zscan4c, Zscan4d, and Zscan4f are almost identical except that one amino acid (I88) in the SCAN-box of Zscan4d is different from the other Zscan4 proteins (Figure S2A), implying that the interaction of Tet2 with Zscan4f could be applicable to other Zscan4 paralogs. Moreover, Zscan4c and Zscan4f have previously been reported to have similar activity for promoting iPSC generation (Jiang et al., 2013). Therefore, we chose Zscan4f, a representative of Zscan4 paralogs, to explore the biological function of the Zscan4-Tet2 complex in establishing the pluripotency.

We expressed FLAG-Zscan4f, FLAG-Zscan4f^{3A}, or the Discosoma red fluorescent protein (dsRed; as a control) in secondary mouse embryonic fibroblast cells carrying four doxycycline (Dox)-inducible Yamanaka factors, namely, Oct4, Sox2, Klf4, and c-Myc (hereinafter referred to as OSKM-2ndMEFs; Figure S3A). We noticed that the expression of four Yamanaka factor genes was comparable at day 4 in Dox-treated cells (D4-OSKM-2ndMEFs; Figure S3B) and that Zscan4f and Zscan4f^{3A} were ectopically expressed at the same levels (Figure S3C). The expression of *Tet* genes was not affected by Zscan4f and Zscan4f^{3A} (Figure 2B). Importantly, the endogenous Tet2 protein was found to interact with overexpressed Zscan4f, but not the Zscan4f^{3A} mutant, in D4-OSKM-2ndMEFs (Figure 2C). In agreement with previously reported functions of Zscan4 in promoting iPSC generation (Hirata et al., 2012; Jiang et al., 2013), we found that forced expression of Zscan4f increased the number of alkaline phosphatase (ALP)-positive colonies by ~3-fold ($p < 0.001$) at day 12, whereas the Zscan4f^{3A} mutant failed to promote reprogramming (Figure 2D), suggesting that the facilitating function of Zscan4f in reprogramming may require Tet2.

To further strengthen the contribution of the Zscan4f-Tet2 complex to reprogramming efficiency rigorously, we retrovirally transduced three Yamanaka factors, Oct4, Sox2, and Klf4 (OSK), as well as either Zscan4f, Zscan4f^{3A}, or dsRed into OG2 MEFs, in which the expression of GFP is driven by the *Oct4* promoter (Figure S3E). Consistently, we found that forced expression of Zscan4f significantly increased the number of GFP-positive colonies by ~10-fold at day 22 (Figures 2E and 2F). All the GFP-positive colonies express SSEA-1 and Rex1, markers for ground state of pluripotency (Figures 2G and S3F). In contrast, forced expression of the Zscan4f^{3A} mutant did not have any effect on iPSC generation (Figures 2D and 2F), confirming that the Tet2 interaction is important for Zscan4f to promote somatic cell reprogramming.

Zscan4f Acts as a Sequence-Specific DNA-Binding TF

Zscan4f contains both the SCAN-box and C_2H_2 zinc finger domain, but there is no reported information regarding the DNA-binding activity and specificity of Zscan4f. To elucidate the genome binding of Zscan4f during reprogramming, we performed chromatin IP followed by deep sequencing in D4-OSKM-2ndMEFs overexpressing FLAG-Zscan4f (GEO: GSE140239). Using the model-based analysis of chromatin immunoprecipitation sequencing (ChIP-seq) (Macs2) peak

Figure 2. Zscan4f Promotes iPSC Generation in a Manner Dependent on Tet2 Interaction

(A) FLAG-Tet2 was transiently co-expressed with hemagglutinin (HA)-tagged Zscan4f or Zscan4f^{3A} in HEK293T cells. The protein-protein interaction was examined by IP-western using indicated antibodies.

(B) Relative *Tet* mRNA levels during early reprogramming in D4-OSKM-2ndMEFs with forced expression of wild-type or Zscan4f^{3A} mutant, as determined by RNA sequencing (RNA-seq).

(C) Endogenous Tet2 interacts with overexpressed Zscan4f, but not Zscan4f^{3A}, in D4-OSKM-2ndMEFs, as determined by IP-western using indicated antibodies.

(D) Zscan4f promotes cell reprogramming in a manner dependent on Tet2 interaction, as determined by counting the ALP-positive colony numbers in D12-OSKM-2ndMEFs with forced expression of Zscan4f or the Zscan4f^{3A} mutant.

(E) Zscan4f promotes iPSC generation in a manner dependent on Tet2 interaction, as determined by counting the GFP-positive colony numbers in D22-OSK-OG2 MEFs with forced expression of Zscan4f or Zscan4f^{3A} mutant.

(F) The kinetics of the reprogramming induced by OSK virus. GFP-positive cells were scored from day 14 to day 22.

(G) Representative images of GFP-positive colonies stained with the anti-SSEA-1 antibody (for pluripotency) and 4′,6-diamidino-2-phenylindole (DAPI; for cell nuclei). Scale bars, 50 μm.

Shown are average values of triplicated results with SEM. ***$p < 0.001$, for the indicated comparison.

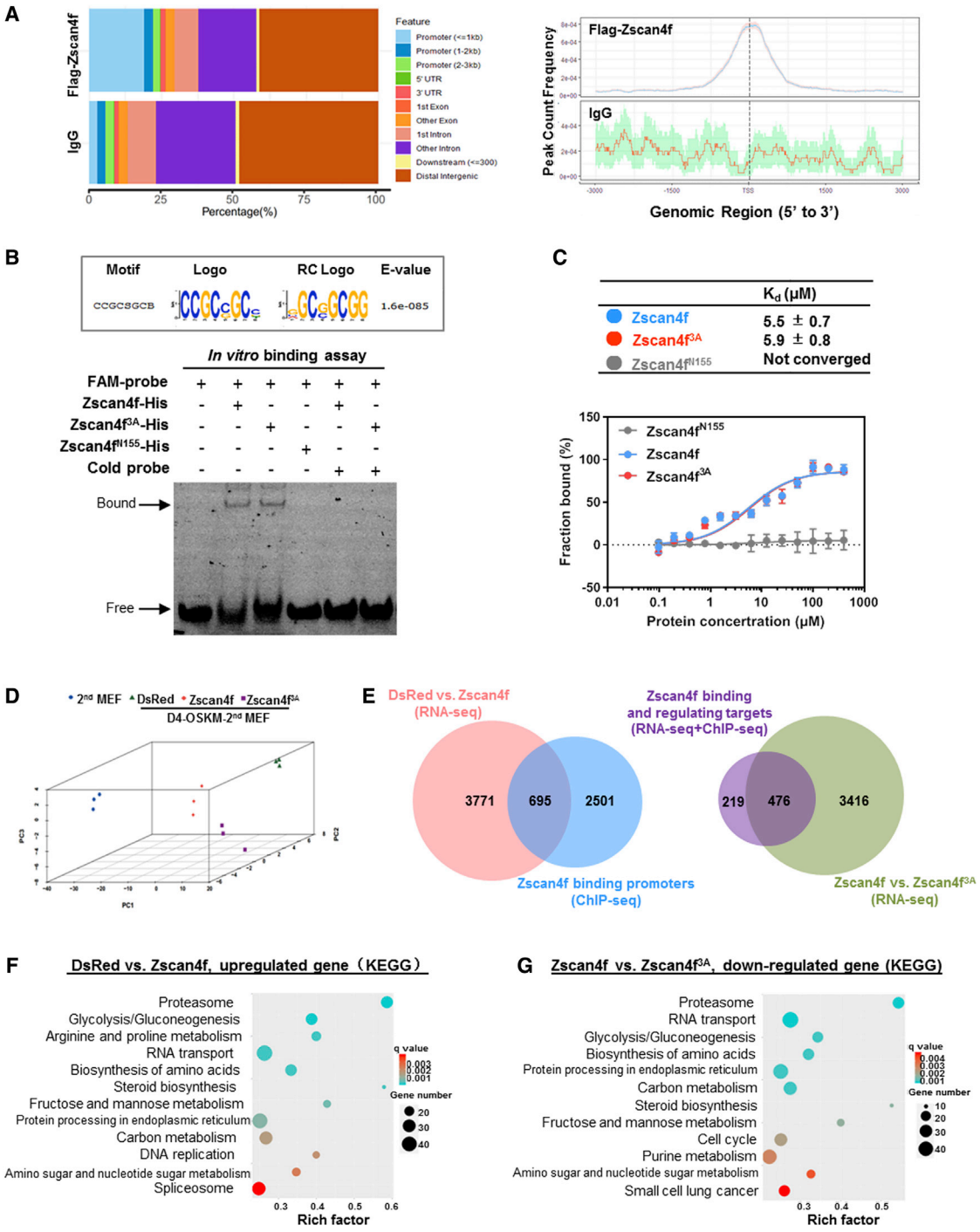

Figure 3. Zscan4f Upregulates Proteasome and Metabolism Genes in a Tet2-Interaction-Dependent Manner

(A) Genomic distribution of FLAG-Zscan4f binding sites in D4-OSKM-2ndMEFs, as determined by ChIP-seq (left). Immunoglobulin G (IgG) was included as a negative control. FLAG-Zscan4f binding peaks are around TSS regions (right).

(B) An octanucleotide motif (CCGCSGCB) as the putative Zscan4f-binding DNA sequence, determined by ChIP-seq (top). *In vitro* EMSA assay was conducted to compare the DNA binding activity of Zscan4f, Zscan4f^{3A}, and Zscan4f^{N155}, and competitive EMSA with unlabeled competitor DNA (referred as cold probe) was also conducted to verify the DNA-binding specificity.

(C) Superimposed fluorescence polarization plots for DNA-binding affinities of Zscan4f, Zscan4f^{3A}, and Zscan4f^{N155}. carboxyfluorescein (FAM)-labeled double-stranded DNA (dsDNA) (15 nM) was incubated with increasing amounts of indicated proteins for 30 min at 25°C in reaction buffer. Fluorescence polarization was measured by the Synergy 4 microplate reader (BioTek) at 25°C, as described in the STAR Methods. Shown are average values of triplicated results with SEM.

(legend continued on next page)

calling method (Zhang et al., 2008), we discovered 10,042 putative Zscan4f-binding sites, of which 3,350 were localized to gene promoters around transcription start site (TSS) regions (Figures 3A and S4A). Gene Ontology (GO) analysis revealed that genes bound by Zscan4f mainly fall into the categories of transcription regulation, chromatin modification, and development-related biological processes, consistent with its reported functions in development-related transcription regulation (Figure S4B).

To further evaluate the chromatin association of Zscan4f, we used discriminative regular expression motif elicitation (DREME) motif search (Bailey, 2011), and predicted an octanucleotide motif (CCGCSGCB) as the putative Zscan4f-binding DNA sequence (E-value = 1.6e-085) (Figure 3B). *In vitro* electrophoretic mobility shift assay (EMSA) showed Zscan4f, but not its SCAN domain (i.e., Zscan4f^{N155}), bound to this DNA motif (Figure 3B). Competitive EMSA with unlabeled competitor DNA (referred as cold probe) confirmed the DNA-binding specificity of Zscan4f (Figure 3B). In addition, EMSA results also demonstrated that the Tet2 protein could not bind to the consensus DNA motif of Zscan4f *in vitro* (Figure S4D), suggesting that Zscan4f recognizes its sequence-specific DNA motif independently of Tet2. Importantly, the Zscan4f^{3A} mutant still bound to the same DNA sequence, indicating that the K73A/E74A/Q75A triple mutations disrupt the Tet2 protein interaction without altering the DNA-binding affinity of Zscan4f. By generating three mutated DNA substrates (e.g., Mut1–3), we found that both Zscan4f and Zscan4f^{3A} mutant failed to bind to Mut1 and Mut2 of the DNA element, but still bound to Mut3 (Figure S4E), indicating the specific sites within the DNA motif that are important for Zscan4f and Zscan4f^{3A} mutant binding. To further quantitatively compare the DNA-binding activity of Zscan4f and Zscan4f^{3A} mutant, we detected the superimposed fluorescence polarization of these two recombinant proteins and found that the Zscan4f^{3A} mutant bound to the same DNA sequence with indistinguishable affinity as wild-type Zscan4f (Figure 3C). These *in vitro* biochemical data thus provide comprehensive characterization for the DNA-binding activity of Zscan4f and Zscan4f^{3A} mutant with defined components and further support that the Tet2-binding-defective Zscan4f^{3A} mutant still binds to the same DNA sequence as wild-type Zscan4f with comparable affinity.

Zscan4f Is an Important Cooperator for Tet2 to Regulate Target Genes

Zscan4 is transiently expressed in preimplantation embryos during zygotic genome activation (ZGA), as well as in a small fraction (1%–5%) of mouse embryonic stem cells (mESCs) resembling 2-cell-stage embryos, referred to as 2C-like state (Amano et al., 2013; Macfarlan et al., 2012; Zalzman et al., 2010). ZGA and 2C-like cells share some common features referred to as Zscan4-associated events or Z4-events, such as rapid heterochromatin derepression and rerepression to maintain genome and chromosome integrity (Ko, 2016). It was previously reported that ectopic expression of *Zscan4* led to increase mRNA expression of many preimplantation-specific genes (Hirata et al., 2012; Jiang et al., 2013). In agreement, we found that multiple preimplantation-specific 2C genes, including *Tcstv1*, *Tcstv3*, *Cphx1*, and *Pat12*, were upregulated in D4-OSKM-2ndMEFs overexpressing Zscan4f (Figure S3D). The expression of those 2C genes was, however, not changed in cells expressing Zscan4f^{3A} mutant (Figure S3D), suggesting that the Zscan4f-Tet2 complex regulates the expression of some preimplantation-specific genes.

It was previously reported that endogenous *Tet2* mRNA expression is induced since day 2 in OSKM-MEFs (Doege et al., 2012) and that Zscan4 is required only for the early stage (first 4 days) to enhance iPSC formation (Hirata et al., 2012). To gain a view of genome-wide transcriptional regulation by the Zscan4f-Tet2 complex, we carried out RNA sequencing in D4-OSKM-2ndMEFs expressing Zscan4f or Zscan4f^{3A} mutant. As expected, the global principal-component analysis (PCA) analysis revealed that MEFs were different from the other three groups of cells with four-Yamanaka-factor induction (Figure 3D). Moreover, we found that forced expression of Zscan4f significantly altered the expression of 4,466 genes ($p < 0.05$; Table S1), including 2,370 upregulated genes, among which the proteasome subunits and enzymes of multiple metabolic pathways were induced most (Figures 3E and 3F). Among Zscan4f-regulating genes, 695 genes were identified as direct targets of Zscan4f by ChIP-seq (Table S2). And a substantial fraction (~68%, 476 of 695 genes) of Zscan4f direct target genes was failed to be regulated by Tet2-binding defective Zscan4f^{3A} mutant (Figure 3E), with those encoding the proteasome subunits and enzymes of multiple metabolic pathways being induced most in the group expressing wild-type Zscan4f, but not in that expressing the Zscan4f^{3A} mutant (Figure 3G).

Thus, these results indicate that Zscan4f acts as an important functional partner of Tet2 to regulate target genes, particularly those encoding glycolytic enzymes and proteasome subunits.

The Zscan4f-Tet2 Complex Regulates Metabolic Rewiring during Reprogramming

Upregulation of glycolytic enzymes promotes reprogramming by enabling a metabolic switch from somatic-cell-preferred oxidative phosphorylation to pluripotent-stem-cell-preferred glycolysis (Folmes et al., 2011; Mathieu et al., 2014; Yoshida et al., 2009; Zhu et al., 2010), but how glycolytic genes are regulated during cell reprogramming is unknown. According to our ChIP-seq data, glucose-metabolism-related genes *Slc2a3* and *Pkm* are the direct target genes of Zscan4f. Moreover, ChIP-qPCR

(D) Global PCA analysis of RNA-seq data among four groups, including 2ndMEFs, D4-OSKM-2ndMEF expressing dsRed, Zscan4f, and Zscan4f^{3A} . Each group contains three biological replicates.

(E) Venn diagrams depicting overlap between the indicated groups in D4-OSKM-2ndMEFs, including the overlap between Zscan4f regulating genes (n = 4466) and Zscan4f binding promoters (n = 3196) (left). Among the overlapped Zscan4f binding and regulating genes (n = 695), 476 genes were failed to be regulated by the Tet2-binding-defective Zscan4f^{3A} mutant (right).

(F) Top GO enrichment analysis of genes that are significantly upregulated by Zscan4f compared to dsRed in D4-OSKM-2ndMEFs.

(G) Top GO enrichment analysis of genes which are significantly downregulated by Zscan4f^{3A} mutant as compared to wild-type Zscan4f in D4-OSKM-2ndMEFs.

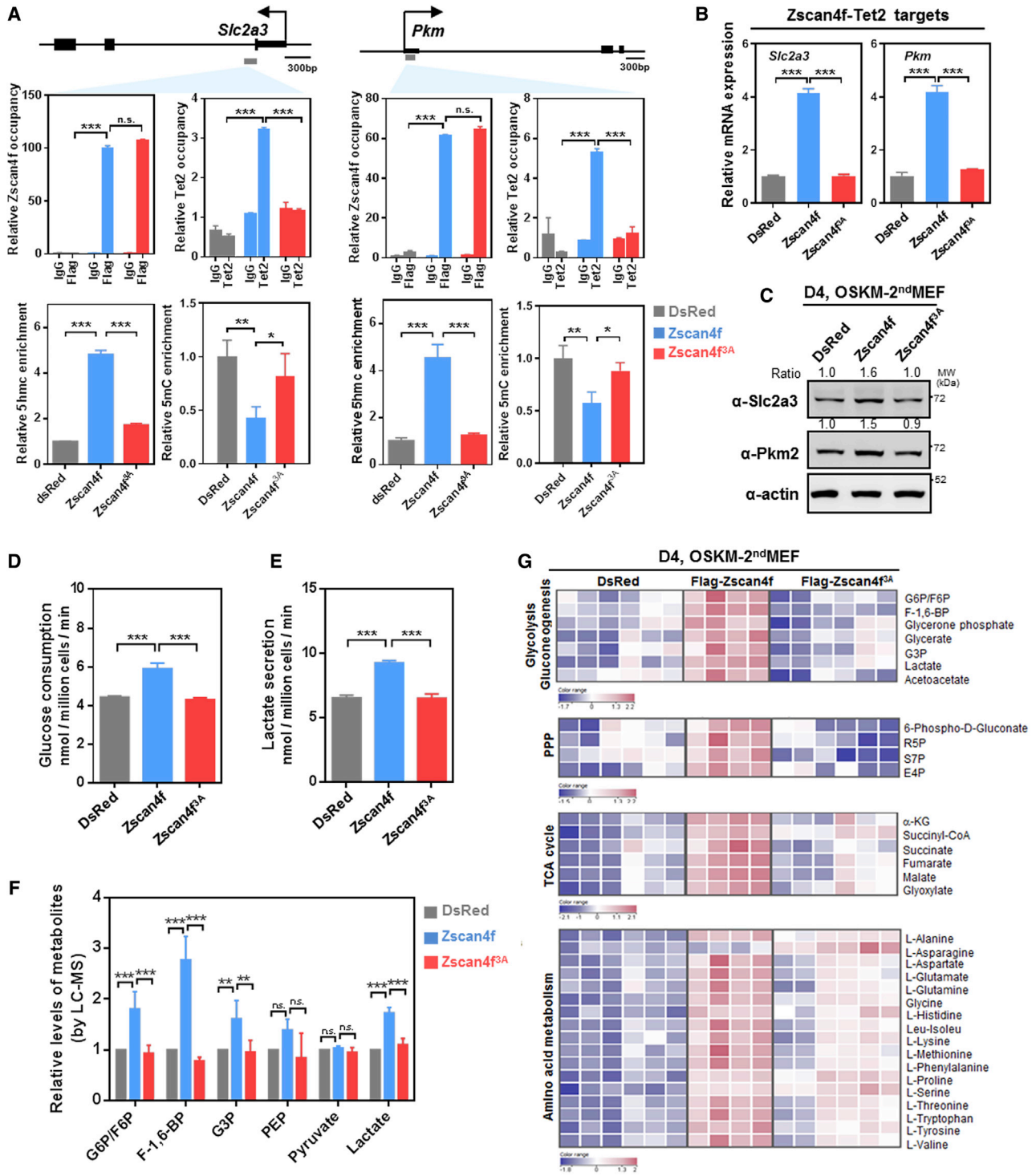

Figure 4. Zscan4f Upregulates Genes Involved in Glucose Metabolism in a Tet2-Interaction-Dependent Manner

(A) Zscan4f, but not the Zscan4f^{3A} mutant, guides Tet2 to facilitate DNA demethylation at the promoter regions of *Slc2a3* and *Pkm* in D4-OSKM-2ndMEFs, as determined by ChIP-qPCR and hMeDIP-qPCR. IgGs were included as negative controls for ChIP-qPCR. Arrow denotes promoter orientation, and CGI (gray line) indicates CpG islands containing Zscan4f-binding motif.

(B) Forced expression of wild-type Zscan4f, but not the Zscan4f^{3A} mutant, upregulates the mRNA expressions of *Slc2a3* and *Pkm* in D4-OSKM-2ndMEFs, as determined by qRT-PCR.

(legend continued on next page)

results revealed that both Zscan4f and Zscan4f^{3A} mutant could bind to the promoter of *Slc2a3* and *Pkm* (Figure 4A). Only Zscan4f, but not Zscan4f^{3A} mutant, could recruit endogenous Tet2 to the promoter regions of *Slc2a3* and *Pkm* in D4-OSKM-2ndMEFs (Figure 4A). The Zscan4f-dependent Tet2 recruitment was associated with increased 5hmC and decreased 5mC at the promoters of *Slc2a3* and *Pkm*, as demonstrated by hydroxylmethylated and methylated DNA IP and quantitative PCR (hMeDIP-qPCR and MeDIP-qPCR, respectively) (Figure 4A). As a result, forced expression of Zscan4f, but not the Zscan4f^{3A} mutant, induced the mRNA and protein expression of Slc2a3 and Pkm (Figures S4C, 4B, and 4C).

Phenotypically, forced expression of Zscan4f, but not the Zscan4f^{3A} mutant, significantly increased glucose consumption and lactate secretion by 1.3-fold ($p < 0.001$) and 1.4-fold ($p < 0.001$), respectively, in D4-OSKM-2ndMEFs (Figures 4D and 4E). Accordingly, intracellular levels of G6P/F6P and lactate in D4-OSKM-2ndMEFs were significantly ($p < 0.01$ or $p < 0.001$) increased by forced expression of Zscan4f, but not the Zscan4f^{3A} mutant (Figure 4F). Furthermore, metabolic profiling analysis confirmed a global metabolic rewiring induced by Zscan4f expression, with 41 metabolites being significantly ($p < 0.05$) altered in glycolysis/gluconeogenesis, pentose phosphate pathway, tricarboxylic acid cycle (TCA) cycle, and amino acid metabolism (Figure 4G; Table S3). Thus, our findings suggest a previously unknown mechanism—recruitment of Tet2 DNA dioxygenase by Zscan4f to activate the expression of metabolic genes—underlying the metabolic switch from oxidative phosphorylation to glycolysis during somatic cell reprogramming.

The Zscan4f-Tet2 Complex Enhances Proteasome Activity during Reprogramming

Another pathway that is most significantly induced by the Zscan4f-Tet2 complex is the proteasome (Figure 3F). Our ChIP-seq analysis identified five genes encoding 26S proteasome subunits as direct targets of Zscan4f, including *Psma2*, *Psma7*, *Psme4*, *Psmd12*, and *Psmd13*. For verification, ChIP-qPCR demonstrated that both Zscan4 and Zscan4f^{3A} mutant were similarly enriched at the promoter regions of non-ATPase regulatory proteasome subunit *Psma7* and *Psmd13* (Figure 5A). Only Zscan4f, but not Zscan4f^{3A} mutant, could recruit endogenous Tet2 to the promoter regions of *Psma7* and *Psmd13* in D4-OSKM-2ndMEFs (Figure 5A). The Zscan4f-dependent Tet2 recruitment was associated with increased 5hmC and decreased 5mC at the promoters of *Psma7* and *Psmd13* (Figure 5A). Consequently, forced expression of Zscan4f, but not Zscan4f^{3A} mutant, upregulated the mRNA expression of 26S proteasome subunits, including *Psma2*, *Psma7*, *Psme4*, *Psmd12*, and *Psmd13* (Figure 5B). Their protein levels were notably increased in D4-OSKM-2ndMEFs expressing Zscan4f, but not Zscan4f^{3A} mutant (Figure 5C), confirming the induction of multiple proteasome subunits by the Zscan4f-Tet2 complex.

To provide functional evidence of increased proteasome gene expression for somatic cell reprogramming, we measured proteasome activity and found that it was increased by 25% ($p < 0.01$) in D4-OSKM-2ndMEFs expressing Zscan4f, but not the Zscan4f^{3A} mutant (Figure 5D). Importantly, we found that treatment of Zscan4f-expressing OSK-OG2 MEFs with two different proteasome inhibitors, bortezomib (BTZ) or MG132, dose-dependently compromises the activity of Zscan4f-induced formation of GFP-positive iPSC colonies without impairing cell proliferation (Figures 5E and 5F). These results suggest that Zscan4f recruits Tet2 to activate the expression of multiple proteasome genes and to increase the proteasome activity, which is functionally important for somatic cell reprogramming.

Conserved Roles of the ZSCAN4-TET2 Transcription Nexus in Regulating Metabolic Rewiring and Proteasome Function

To clarify whether the regulatory function of the Zscan4f-Tet2 interaction is conserved across species, we next investigated whether or not the ZSCAN4-TET2 complex could similarly regulate proteasome and metabolic genes during reprogramming of human somatic cells. When it is co-expressed in HEK293T cells, we found that the SCAN-box of human ZSCAN4 interacted with full-length TET2 through the Cys-rich and double-stranded β-helix (DSBH) dioxygenase domains (Figures 6A and S5A). Given that the Cys-rich and DSBH domains are conserved in all three TET proteins, it is possible that ZSCAN4 may also interact with TET1 and TET3, in addition to TET2. To further elucidate this question, we performed a co-IP assay and found that the SCAN domain of ZSCAN4 (ZSCAN4^{N168}) interacted with mouse TET1 and human TET3 (lacking CXXC domain) (Figure S5B).

On the basis of sequence alignments of human SCAN family members, we focused on conserved regions (while excluding the residues involved in SCAN dimerization) and carried out a systematic mutagenesis screen to map residues important for TET2 binding. Eventually, we identified two residues in the SCAN-box of ZNF444 (i.e., L49 and P73), each mutated to alanine, partially reduced the association with TET2 (Figures S5C, S5D, and S5E). The mutation sites of L49 and P73 in the SCAN domain of ZNF444 are equal to L73 and H97 in the SCAN-box of ZSCAN4 (Figure S5C). H97 in ZSCAN4 is,

(C) Forced expression of wild-type Zscan4f, but not the Zscan4f^{3A} mutant, increases the protein expression of Slc2a3 and Pkm in D4-OSKM-2ndMEFs, as determined by western blot. Relative Slc2a3 and Pkm protein levels were normalized against β-actin protein. Shown are representative results.
(D and E) Forced expression of wild-type Zscan4f, but not the Zscan4f^{3A} mutant, increases glucose consumption (D) and promotes lactate secretion (E) in D4-OSKM-2ndMEFs, as determined by using the glucose or lactate assay kit as described in the STAR Methods.
(F) Forced expression of wild-type Zscan4f, but not the Zscan4f^{3A} mutant, increases the intracellular levels of several glycolytic intermediates in D4-OSKM-2ndMEFs, as determined by liquid chromatography-tandem mass spectrometry (LC-MS/MS) analysis as described in the STAR Methods.
(G) Metabolic profiling analysis shows global metabolic rewiring induced by forced expression of wild-type Zscan4f, but not the Zscan4f^{3A} mutant. Heatmap of metabolites detected in D4-OSKM-2ndMEFs from selected metabolic pathways. Each line represents a metabolite detected by LC-MS/MS analysis, and values are represented as the metabolite: internal standard area ratio of MS signals detected by multiple reaction monitoring (MRM) and is normalized by cell numbers. Columns represent each biological replicate. The colors vary from deep blue (very low data value) to dark red (extremely high data value).
Shown are average values of triplicated results with SEM. *$p < 0.05$; **$p < 0.01$; ***$p < 0.001$ for the indicated comparison. n.s., not significant.

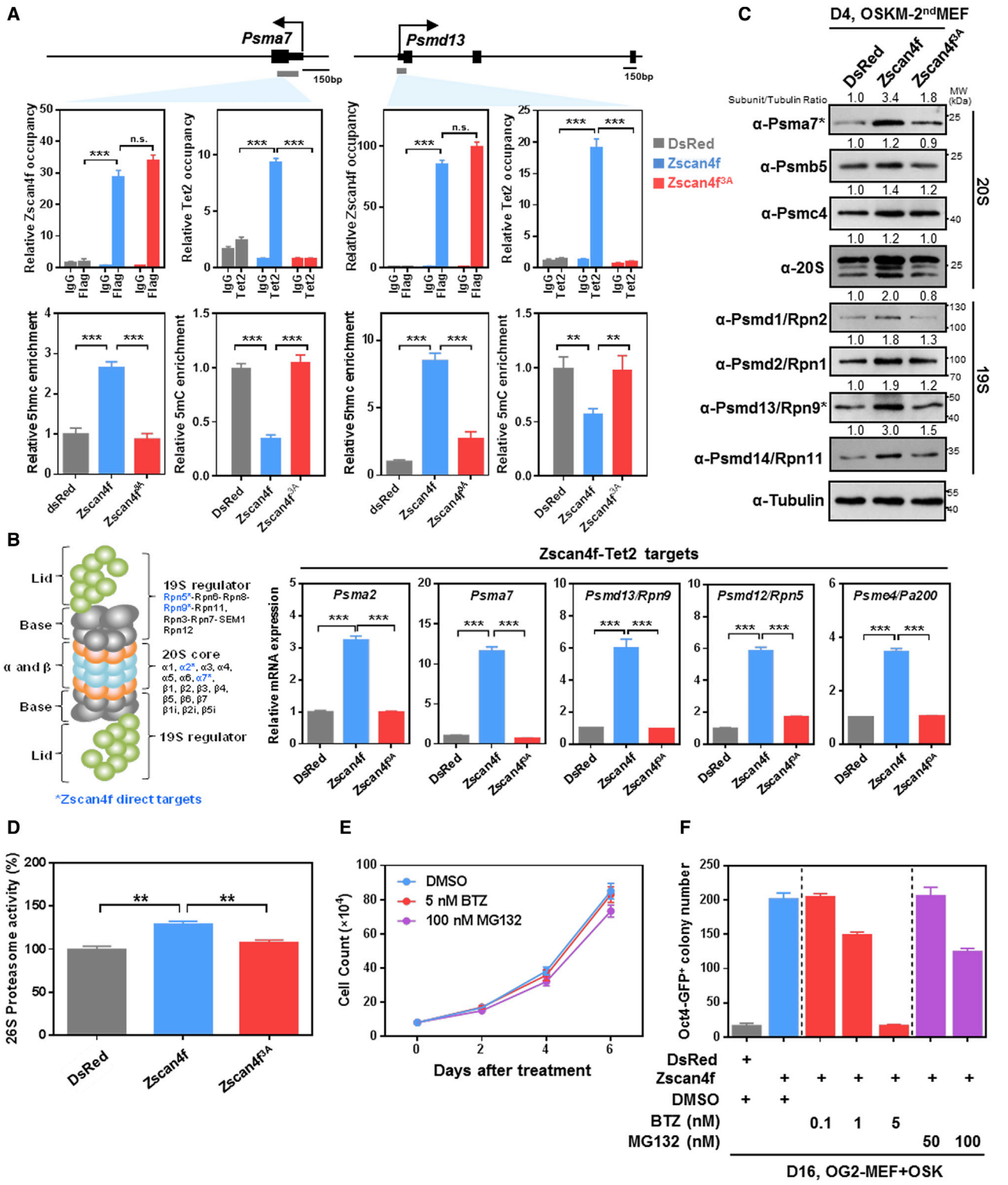

Figure 5. Zscan4f-Tet2 Interaction Increases Proteasome Expression and Function during Reprogramming

(A) Zscan4f, but not the Zscan4f^{3A} mutant, guides Tet2 to facilitate DNA demethylation at the promoter regions of *Psma7* and *Psmd13* in D4-OSKM-2ndMEFs, as determined by ChIP-qPCR and hMeDIP-qPCR. IgGs were included as negative controls for ChIP-qPCR. Arrow denotes promoter orientation, and tCGI (gray line) indicates CpG islands containing Zscan4f-binding motif.

(legend continued on next page)

however, not conserved as the corresponding proline (P) residue in ZNF444 and other ZSCAN family members. We found that a mutation of L73A (referred to as ZSCAN4^{mut}), but not H97A, in the SCAN-box of ZSCAN4 completely disrupted its association with TET2 (Figure 6B), suggesting that the highly conserved residue L73 in the SCAN domain of ZSCAN4 is crucial for TET2 interaction.

Finally, to evaluate the function of the ZSCAN4-TET2 interaction during reprogramming, we introduced four Yamanaka factors into human fetal lung fibroblasts MRC-5 (ATCC, CCL-171) together with the empty vector, FLAG-ZSCAN4, or FLAG-ZSCAN4^{mut}, followed by determination of gene expression at day 7 post-infection (Figure S6). In accordance with our observations in mouse fibroblast reprogramming, forced expression of wild-type ZSCAN4, but not ZSCAN4^{mut}, significantly ($p < 0.001$) upregulated the mRNA expression of proteasome and glucose metabolism genes in D7-OSKM-CCL-171 cells (Figure 6C). As a result, the 26S proteasome activity was significantly increased by 15% ($p < 0.01$) in cells expressing ZSCAN4 but remained unchanged in cells expressing ZSCAN4^{mut} (Figure 6D). Moreover, forced expression of wild-type ZSCAN4, but not ZSCAN4^{mut}, significantly increased glucose consumption and lactate secretion by 1.4-fold ($p < 0.001$) and 1.3-fold ($p < 0.001$), respectively, in D7-OSKM-CCL-171 cells (Figures 6E and 6F). In addition, ZSCAN4, but not ZSCAN4^{mut}, could promote the phenotype of mesenchymal-to-epithelial transition (MET), a requisite step bridging iPSC reprogramming (Figure S6). Collectively, these results reveal a previously unrecognized and conserved function of the ZSCAN4-TET2 complex to regulate proteasome activity and cellular metabolism to initiate the reprogramming.

DISCUSSION

As a characteristic marker for the 2C-like state, Zscan4 is expressed exclusively in late 2C embryos and transiently in mESCs. Knockdown of *Zscan4* in 2C embryos delays embryo development for a day and blocks blastocysts to implant (Falco et al., 2007; Zalzman et al., 2010). In mESCs, continuously knocking down *Zscan4* over a period of multiple passages (>6) reduces cell proliferation and causes cell death accompanied by massive karyotype abnormality (Zalzman et al., 2010). On the other hand, ectopic expression of Zscan4 transiently activates early embryonic genes, including many preimplantation-specific genes, and promotes somatic cell reprogramming toward pluripotency (Hirata et al., 2012; Jiang et al., 2013). Here, we show that forced expression of Zscan4f, but not the Zscan4f^{3A} mutant, upregulates several preimplantation-specific 2C genes (e.g., *Tcstv1/3*, *Cphx1*, and *Pat12*) at the early phase of iPSC formation. In fact, *Tcstv1* is a direct target of Zscan4f, whereas the other tested preimplantation-specific genes contain no Zscan4f-binding motifs within their promoter regions (data not shown). Thus, preimplantation-specific genes are transcriptionally regulated by the Zscan4f-Tet2 complex by both direct and indirect mechanisms.

Our current study has identified a biochemical mechanism of Zscan4—binding to and recruiting the Tet2 enzyme to promote DNA demethylation and induce expression of target genes, particularly those encoding glycolytic enzymes and proteasome subunits. Our *in vitro* assay results clearly demonstrate that the Zscan4f^{3A} mutant binds to the same DNA sequence as wild-type Zscan4f with comparable affinity but loses the ability to interact with Tet2. Additionally, the use of ChIP-seq to detect the binding sites of the Zscan4f^{3A} mutant across the genome is needed to further support this conclusion. Notably, we show a substantial fraction (~68%, 476 of 695) of Zscan4f direct target genes is unable to be regulated by the Tet2-binding-defective Zscan4f^{3A} mutant, suggesting that Tet2 acts through interacting with Zscan4f, which binds to DNA motifs and regulates gene expression. Mechanistically, Zscan4f and Tet2 co-occupy at the promoter regions of target genes that modulate glycolysis and proteasome activity. The switch from OXPHO to a glycolysis-based metabolism has previously been reported to be important for somatic cell reprogramming (Folmes et al., 2011; Panopoulos et al., 2012; Zhu et al., 2010). Our results show that Zscan4f recruits Tet2 to promote the DNA demethylation and transcription activation of glycolytic genes, which enable a metabolic switch into a Warburg-like glycolytic metabotype. On the other hand, protein homeostasis is central for self-renewal, pluripotency, and cell fate decisions (García-Prat et al., 2017). Supporting this notion, human ESCs, mESCs, and iPSC cells exhibit increased proteasome activity compared with their differentiated counterparts (Hernebring et al., 2006; Vilchez et al., 2012). However, there is a profound lack of knowledge on the regulation of proteasome expression and activity. In our study, we show that the Zscan4f-Tet2 complex activates the expression of proteasome subunit genes, re-affirming that Zscan4f acts as an important partner of Tet2 to regulate target genes. Strikingly, a partial reduction of the proteasome activity blunted the Zscan4f-induced formation of iPSC colonies without impairing cell growth, indicating the critical importance of Zscan4f-Tet2-induced proteasome activity for somatic cell reprogramming. We propose that metabolic rewiring and enhanced proteostasis activity are all part of an essential

(B) Schematic diagram of proteasome subunits (left). According to our ChIP-seq data, five proteasome genes are direct targets of Zscan4f (marked with * in blue), including *Psma2*, *Psma7*, *Psmd12/Rpn5*, *Psmd13/Rpn9*, and *Psme4/Pa200* (not shown). Forced expression of wild-type Zscan4f, but not the Zscan4f^{3A} mutant, was found to upregulate the mRNA expressions of multiple proteasome subunits in D4-OSKM-2ndMEFs, as determined by qRT-PCR.

(C) Forced expression of wild-type Zscan4f, but not the Zscan4f^{3A} mutant, increases the protein expression of indicated proteasome subunits in D4-OSKM-2ndMEFs, as determined by western blot. Relative protein levels of proteasome subunits were normalized against the Tubulin protein. Shown are representative results.

(D) Forced expression of wild-type Zscan4f, but not the Zscan4f^{3A} mutant, increases the proteasome activity in D4-OSKM-2ndMEFs, as determined by using the substrate (LLVY-AMC for chymotrypsin-like activity) as described in the STAR Methods.

(E and F) Treatment with proteasome inhibitors compromises the effect of Zscan4f on promoting iPSC generation without impairing cell proliferation. Zscan4f-overexpressing OSK-OG2 MEFs were treated with the indicated concentrations of MG132 or bortezomib (BTZ), following cell number counting for 6 days (E) as well as the GFP-positive colony counting at day 16 (F).

(F) Shown are average values of triplicated results with SEM. $^{**}p < 0.01$; $^{***}p < 0.001$ for the indicated comparison.

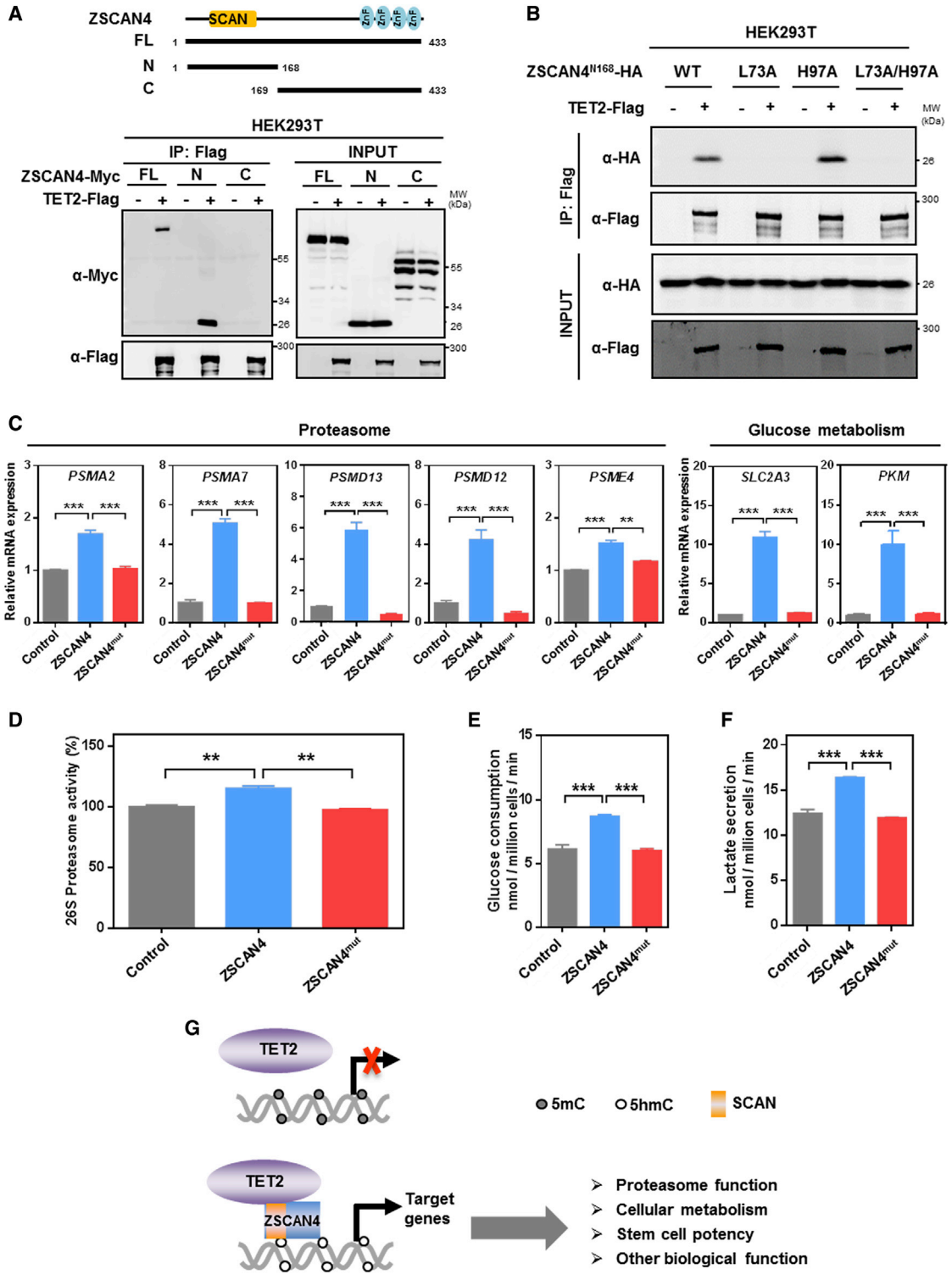

Figure 6. ZSCAN4 Interacts with TET2 to Induce Proteasome and Glycolytic Genes

(A) Structural features of human ZSCAN4 and truncated proteins (top). FLAG-TET2 was transiently co-expressed with Myc-tagged FL ZSCAN4 or truncations in HEK293T cells. The truncated proteins of ZSCAN4 include N (N-terminal 1–168 amino acid [aa], containing the SCAN-box) and C (C-terminal 169–433 aa). Protein-protein interaction was examined by IP-western using the indicated antibodies.

(B) FLAG-TET2 was transiently co-expressed with the indicated HA-tagged wild-type or mutant ZSCAN4 in HEK293T cells. Protein-protein interaction was examined by IP-western using the indicated antibodies.

(legend continued on next page)

program coordinated by the Zscan4-Tet2 transcription nexus to orchestrate the establishment and maintenance of pluripotency (Figure 6G). In addition to iPSC reprogramming, Zscan4 has been shown to promote genomic stability and dramatically improve the quality of iPSCs (Jiang et al., 2013). Whether Zscan4 and Tet2 work synergistically to improve the pluripotency of iPSC is a potentially interesting topic and needs further investigation in genetic mouse models.

To evaluate the function of the ZSCAN4-TET2 complex on human somatic cell reprogramming, we have tried to induce human iPSC generation by using immortalized CCL-171 cells, as previously reported (Chambers et al., 2009; Park et al., 2017). We found that the human cell reprogramming took much time and the efficiency was extremely low, especially for those where multiple viruses were used for iPSC induction. Nevertheless, our results show that forced expression of ZSCAN4, but not the TET2-binding-defective mutant, can induce the expression of genes encoding glycolytic enzymes and proteasome subunits and can promote the cellular MET phenotype, a requisite step bridging successful iPSC reprogramming. This result, at least in part, suggests that ZSCAN4 plays a positive role in initiating reprogramming in a TET2-interaction-dependent manner. Further investigation is needed to explore the relevant function/implication of ZSCAN4, TET2, and their interaction in the establishment of human cellular reprogramming.

Except for ZSCAN4, we have demonstrated that at least 19 additional ZSCAN proteins can interact with TET2. Of note, L73 in the SCAN-box of ZSCAN4 is highly conserved among human ZSCAN proteins, suggesting a conserved feature of the SCAN-TET2 interaction may exist among different ZSCAN proteins. On the other hand, the SCAN-box interacts with the Cys-rich and DSBH dioxygenase domains of TET2, which are highly conserved among three TET family members. Considering that the SCAN domains mediate heterodimerization with other SCAN domains, our findings thus suggest that recruiting TET dioxygenases to target genes may represent a general mechanism, underlying the function of the ZSCAN family of TFs to regulate diverse cellular processes, including reprogramming.

STAR★METHODS

Detailed methods are provided in the online version of this paper and include the following:

- KEY RESOURCES TABLE
- RESOURCE AVAILABILITY
  - Lead Contact
  - Materials Availability
  - Data and Code Availability
- EXPERIMENTAL MODEL AND SUBJECT DETAILS
  - Animals
  - Cell lines
  - Primary cell cultures
- METHOD DETAILS
  - Mammalian two-hybrid assay
  - Transfection and immunoprecipitation
  - *In vitro* pull-down assay
  - EMSA assay
  - Fluorescence polarization assay
  - RNA isolation and qRT-PCR analysis
  - RNA-seq assay
  - ChIP-seq assay
  - Chromatin Immunoprecipitation (ChIP)-qPCR assay
  - hMeDIP-qPCR and MeDIP-qPCR analysis
  - Somatic cell reprogramming and iPSC generation
  - ALP staining
  - Immunofluorescence assay
  - Measurement of glucose consumption and lactate secretion
  - Metabolite profiling by LC-MS/MS
  - Proteasome activity assay
- QUANTIFICATION AND STATISTICAL ANALYSIS

SUPPLEMENTAL INFORMATION

Supplemental Information can be found online at https://doi.org/10.1016/j.celrep.2020.107877.

ACKNOWLEDGMENTS

We thank members of the Molecular and Cell Biology laboratory of Fudan University for discussions and support throughout this study. We are grateful for the kind offer of pMXs-Zscan4f-FLAG and OG2 transgenic mice from Dr. Jingsong Li (Chinese Academy of Sciences, Shanghai) and Myc-tagged human TET3 from Dr. Jiemin Wong (East China Normal University). This work was supported by the National Key R&D Program of China (no. 2016YFA0501800 to D.Y.), NSFC grants (no. 31871431 and 31821002 to D.Y., no. 31771643 to M.Z., no. 81572256 to P.-Y.L., and no. 31671391 to X.G.), the Innovative research team of high-level local universities in Shanghai (to D.Y. and M.Z.), the Incentive Project of High-level Innovation Team for Shanghai Jiao Tong University School of Medicine (to M.Z.), the Shanghai Pujiang Program (17PJ1405200 to M.Z.), the Program for Professor of Special Appointment (Eastern Scholar) at Shanghai Institutions of Higher Learning (to M.Z.), the Shanghai Science and Technology Committee (19JC1413200 to M.Z.), funding from the Shanghai Key Laboratory of Reproductive Medicine (to M.Z.), and the Zhejiang Natural Science Foundation (no. LR18C050001 to G.X.).

AUTHOR CONTRIBUTIONS

Z.-L.C., K.-L.G., Y. Xiong, and D.Y. conceived the general framework of this study. Z.-L.C., M.-L.Z., and D.Y. designed the experiments. Z.-L.C., M.-L.Z.,

(C) Forced expression of wild-type ZSCAN4, but not the TET2-binding defective mutant, upregulates the mRNA expression of indicated genes in D7-OSKM-CCL-171 cells, as determined by qRT-PCR.
(D) Forced expression of wild-type ZSCAN4, but not the TET2-binding defective mutant, increases the proteasome activity in D7-OSKM-CCL-171 cells, as determined by using the substrate (LLVY-AMC for chymotrypsin-like activity), as described in the STAR Methods.
(E and F) Forced expression of wild-type ZSCAN4, but not the TET2-binding defective mutant, increases glucose consumption (E) and promotes lactate secretion (F) in D7-OSKM-CCL-171 cells, as determined by using the glucose or lactate assay kit as described in the STAR Methods. Shown are average values of triplicated results with SEM. $^{**}p < 0.01$; $^{***}p < 0.001$ for the indicated comparison.
(G) Working model. TET2 interacts with ZSCAN family proteins through the SCAN domain and regulates ZSCAN4-associated events, such as cellular metabolism, proteasome function, and iPSC generation during reprogramming.

H.-P.L., C.G., J.-B.S., Z.Z., L.L., Y.Z., X.S., H.Z., Z.H., W.Z., and C.Z. performed experiments. H.-P.L. and M.-L.Z. established the mammalian two-hybrid screen assay. Z.H. and Z.Z. guided and analyzed the ChIP-seq data. Y.Z. and X.S. detected the 26S proteasome activity. Z.-L.C., M.-L.Z., and D.Y. prepared the manuscript.

DECLARATION OF INTERESTS

The authors declare no competing interests.

Received: November 8, 2019
Revised: February 4, 2020
Accepted: June 16, 2020
Published: July 14, 2020

REFERENCES

Amano, T., Hirata, T., Falco, G., Monti, M., Sharova, L.V., Amano, M., Sheer, S., Hoang, H.G., Piao, Y., Stagg, C.A., et al. (2013). Zscan4 restores the developmental potency of embryonic stem cells. Nat. Commun. *4*, 1966.

Bailey, T.L. (2011). DREME: motif discovery in transcription factor ChIP-seq data. Bioinformatics *27*, 1653–1659.

Chambers, S.M., Fasano, C.A., Papapetrou, E.P., Tomishima, M., Sadelain, M., and Studer, L. (2009). Highly efficient neural conversion of human ES and iPS cells by dual inhibition of SMAD signaling. Nat. Biotechnol. *27*, 275–280.

Chen, L.L., Lin, H.P., Zhou, W.J., He, C.X., Zhang, Z.Y., Cheng, Z.L., Song, J.B., Liu, P., Chen, X.Y., Xia, Y.K., et al. (2018). SNIP1 Recruits TET2 to Regulate c-MYC Target Genes and Cellular DNA Damage Response. Cell Rep. *25*, 1485–1500.e1484.

Costa, Y., Ding, J., Theunissen, T.W., Faiola, F., Hore, T.A., Shliaha, P.V., Fidalgo, M., Saunders, A., Lawrence, M., Dietmann, S., et al. (2013). NANOG-dependent function of TET1 and TET2 in establishment of pluripotency. Nature *495*, 370–374.

de la Rica, L., Rodríguez-Ubreva, J., García, M., Islam, A.B., Urquiza, J.M., Hernando, H., Christensen, J., Helin, K., Gómez-Vaquero, C., and Ballestar, E. (2013). PU.1 target genes undergo Tet2-coupled demethylation and DNMT3b-mediated methylation in monocyte-to-osteoclast differentiation. Genome Biol. *14*, R99.

Doege, C.A., Inoue, K., Yamashita, T., Rhee, D.B., Travis, S., Fujita, R., Guarnieri, P., Bhagat, G., Vanti, W.B., Shih, A., et al. (2012). Early-stage epigenetic modification during somatic cell reprogramming by Parp1 and Tet2. Nature *488*, 652–655.

Edelstein, L.C., and Collins, T. (2005). The SCAN domain family of zinc finger transcription factors. Gene *359*, 1–17.

Emerson, R.O., and Thomas, J.H. (2011). Gypsy and the birth of the SCAN domain. J. Virol. *85*, 12043–12052.

Falco, G., Lee, S.L., Stanghellini, I., Bassey, U.C., Hamatani, T., and Ko, M.S. (2007). Zscan4: a novel gene expressed exclusively in late 2-cell embryos and embryonic stem cells. Dev. Biol. *307*, 539–550.

Fidalgo, M., Huang, X., Guallar, D., Sanchez-Priego, C., Valdes, V.J., Saunders, A., Ding, J., Wu, W.S., Clavel, C., and Wang, J. (2016). Zfp281 Coordinates Opposing Functions of Tet1 and Tet2 in Pluripotent States. Cell Stem Cell *19*, 355–369.

Folmes, C.D., Nelson, T.J., Martinez-Fernandez, A., Arrell, D.K., Lindor, J.Z., Dzeja, P.P., Ikeda, Y., Perez-Terzic, C., and Terzic, A. (2011). Somatic oxidative bioenergetics transitions into pluripotency-dependent glycolysis to facilitate nuclear reprogramming. Cell Metab. *14*, 264–271.

García-Prat, L., Sousa-Victor, P., and Muñoz-Cánoves, P. (2017). Proteostatic and Metabolic Control of Stemness. Cell Stem Cell *20*, 593–608.

Guallar, D., Bi, X., Pardavila, J.A., Huang, X., Saenz, C., Shi, X., Zhou, H., Faiola, F., Ding, J., Haruehanroengra, P., et al. (2018). RNA-dependent chromatin targeting of TET2 for endogenous retrovirus control in pluripotent stem cells. Nat. Genet. *50*, 443–451.

Guo, X., Wang, L., Li, J., Ding, Z., Xiao, J., Yin, X., He, S., Shi, P., Dong, L., Li, G., et al. (2015). Structural insight into autoinhibition and histone H3-induced activation of DNMT3A. Nature *517*, 640–644.

He, Y.F., Li, B.Z., Li, Z., Liu, P., Wang, Y., Tang, Q., Ding, J., Jia, Y., Chen, Z., Li, L., et al. (2011). Tet-mediated formation of 5-carboxylcytosine and its excision by TDG in mammalian DNA. Science *333*, 1303–1307.

Hernebring, M., Brolén, G., Aguilaniu, H., Semb, H., and Nyström, T. (2006). Elimination of damaged proteins during differentiation of embryonic stem cells. Proc. Natl. Acad. Sci. USA *103*, 7700–7705.

Hirata, T., Amano, T., Nakatake, Y., Amano, M., Piao, Y., Hoang, H.G., and Ko, M.S. (2012). Zscan4 transiently reactivates early embryonic genes during the generation of induced pluripotent stem cells. Sci. Rep. *2*, 208.

Ito, S., D'Alessio, A.C., Taranova, O.V., Hong, K., Sowers, L.C., and Zhang, Y. (2010). Role of Tet proteins in 5mC to 5hmC conversion, ES-cell self-renewal and inner cell mass specification. Nature *466*, 1129–1133.

Ito, S., Shen, L., Dai, Q., Wu, S.C., Collins, L.B., Swenberg, J.A., He, C., and Zhang, Y. (2011). Tet proteins can convert 5-methylcytosine to 5-formylcytosine and 5-carboxylcytosine. Science *333*, 1300–1303.

Iyer, L.M., Tahiliani, M., Rao, A., and Aravind, L. (2009). Prediction of novel families of enzymes involved in oxidative and other complex modifications of bases in nucleic acids. Cell Cycle *8*, 1698–1710.

Jiang, J., Lv, W., Ye, X., Wang, L., Zhang, M., Yang, H., Okuka, M., Zhou, C., Zhang, X., Liu, L., and Li, J. (2013). Zscan4 promotes genomic stability during reprogramming and dramatically improves the quality of iPS cells as demonstrated by tetraploid complementation. Cell Res. *23*, 92–106.

Ko, M.S. (2016). Zygotic Genome Activation Revisited: Looking Through the Expression and Function of Zscan4. Curr. Top. Dev. Biol. *120*, 103–124.

Ko, M., An, J., Bandukwala, H.S., Chavez, L., Aijö, T., Pastor, W.A., Segal, M.F., Li, H., Koh, K.P., Lähdesmäki, H., et al. (2013). Modulation of TET2 expression and 5-methylcytosine oxidation by the CXXC domain protein IDAX. Nature *497*, 122–126.

Kohli, R.M., and Zhang, Y. (2013). TET enzymes, TDG and the dynamics of DNA demethylation. Nature *502*, 472–479.

Lan, F., Collins, R.E., De Cegli, R., Alpatov, R., Horton, J.R., Shi, X., Gozani, O., Cheng, X., and Shi, Y. (2007). Recognition of unmethylated histone H3 lysine 4 links BHC80 to LSD1-mediated gene repression. Nature *448*, 718–722.

Macfarlan, T.S., Gifford, W.D., Driscoll, S., Lettieri, K., Rowe, H.M., Bonanomi, D., Firth, A., Singer, O., Trono, D., and Pfaff, S.L. (2012). Embryonic stem cell potency fluctuates with endogenous retrovirus activity. Nature *487*, 57–63.

Mathieu, J., Zhou, W., Xing, Y., Sperber, H., Ferreccio, A., Agoston, Z., Kuppusamy, K.T., Moon, R.T., and Ruohola-Baker, H. (2014). Hypoxia-inducible factors have distinct and stage-specific roles during reprogramming of human cells to pluripotency. Cell Stem Cell *14*, 592–605.

Nam, K., Honer, C., and Schumacher, C. (2004). Structural components of SCAN-domain dimerizations. Proteins *56*, 685–692.

Panopoulos, A.D., Yanes, O., Ruiz, S., Kida, Y.S., Diep, D., Tautenhahn, R., Herrerías, A., Batchelder, E.M., Plongthongkum, N., Lutz, M., et al. (2012). The metabolome of induced pluripotent stem cells reveals metabolic changes occurring in somatic cell reprogramming. Cell Res. *22*, 168–177.

Park, S.J., Lee, S.A., Prasain, N., Bae, D., Kang, H., Ha, T., Kim, J.S., Hong, K.S., Mantel, C., Moon, S.H., et al. (2017). Metabolome Profiling of Partial and Fully Reprogrammed Induced Pluripotent Stem Cells. Stem Cells Dev. *26*, 734–742.

Peterson, F.C., Hayes, P.L., Waltner, J.K., Heisner, A.K., Jensen, D.R., Sander, T.L., and Volkman, B.F. (2006). Structure of the SCAN domain from the tumor suppressor protein MZF1. J. Mol. Biol. *363*, 137–147.

Sardina, J.L., Collombet, S., Tian, T.V., Gómez, A., Di Stefano, B., Berenguer, C., Brumbaugh, J., Stadhouders, R., Segura-Morales, C., Gut, M., et al. (2018). Transcription Factors Drive Tet2-Mediated Enhancer Demethylation to Reprogram Cell Fate. Cell Stem Cell *23*, 905–906.

Tahiliani, M., Koh, K.P., Shen, Y., Pastor, W.A., Bandukwala, H., Brudno, Y., Agarwal, S., Iyer, L.M., Liu, D.R., Aravind, L., and Rao, A. (2009). Conversion

of 5-methylcytosine to 5-hydroxymethylcytosine in mammalian DNA by MLL partner TET1. Science *324*, 930–935.

Vilchez, D., Boyer, L., Morantte, I., Lutz, M., Merkwirth, C., Joyce, D., Spencer, B., Page, L., Masliah, E., Berggren, W.T., et al. (2012). Increased proteasome activity in human embryonic stem cells is regulated by PSMD11. Nature *489*, 304–308.

Wang, Y., Xiao, M., Chen, X., Chen, L., Xu, Y., Lv, L., Wang, P., Yang, H., Ma, S., Lin, H., et al. (2015). WT1 recruits TET2 to regulate its target gene expression and suppress leukemia cell proliferation. Mol. Cell *57*, 662–673.

Williams, A.J., Khachigian, L.M., Shows, T., and Collins, T. (1995). Isolation and characterization of a novel zinc-finger protein with transcription repressor activity. J. Biol. Chem. *270*, 22143–22152.

Xiong, J., Zhang, Z., Chen, J., Huang, H., Xu, Y., Ding, X., Zheng, Y., Nishinakamura, R., Xu, G.L., Wang, H., et al. (2016). Cooperative Action between SALL4A and TET Proteins in Stepwise Oxidation of 5-Methylcytosine. Mol. Cell *64*, 913–925.

Yoshida, Y., Takahashi, K., Okita, K., Ichisaka, T., and Yamanaka, S. (2009). Hypoxia enhances the generation of induced pluripotent stem cells. Cell Stem Cell *5*, 237–241.

Zalzman, M., Falco, G., Sharova, L.V., Nishiyama, A., Thomas, M., Lee, S.L., Stagg, C.A., Hoang, H.G., Yang, H.T., Indig, F.E., et al. (2010). Zscan4 regulates telomere elongation and genomic stability in ES cells. Nature *464*, 858–863.

Zhang, Y., Liu, T., Meyer, C.A., Eeckhoute, J., Johnson, D.S., Bernstein, B.E., Nusbaum, C., Myers, R.M., Brown, M., Li, W., and Liu, X.S. (2008). Model-based analysis of ChIP-Seq (MACS). Genome Biol. *9*, R137.

Zhao, B., Ye, X., Yu, J., Li, L., Li, W., Li, S., Yu, J., Lin, J.D., Wang, C.Y., Chinnaiyan, A.M., et al. (2008). TEAD mediates YAP-dependent gene induction and growth control. Genes Dev. *22*, 1962–1971.

Zhu, S., Li, W., Zhou, H., Wei, W., Ambasudhan, R., Lin, T., Kim, J., Zhang, K., and Ding, S. (2010). Reprogramming of human primary somatic cells by OCT4 and chemical compounds. Cell Stem Cell *7*, 651–655.

STAR★METHODS

KEY RESOURCES TABLE

REAGENT or RESOURCE	SOURCE	IDENTIFIER
Antibodies		
Tet2 for western-blot and chromatin immunoprecipitation	CST	Cat#92529
TET2 for immunoprecipitation	YouKe Biotechnology	Immunogen: 1-232 aa of TET2
TET2 for western-blot	Abclonal	Cat#A1526
Flag tag	Shanghai Genomics Technology	Cat#4110-20
Myc tag	HuaAn Biological Technology	Cat#R1208-1
HA tag	HuaAn Biological Technology	Cat#ET1611-49
Gal4	Santa Cruz	Cat#sc-510
5hmC	Active Motif	Cat#39769
5mC	Active Motif	Cat#39649
Slc2a3	Proteintech	Cat#20403-1-AP
Pkm	CST	Cat#4053T
SSEA-1	R&D	Cat#MAB2155
Rpn1 (PSMD2)	Santa Cruz	Cat#sc-271775
Rpn2 (PSMD1)	Santa Cruz	Cat#sc-166038
Rpn9 (PSMD13)	Abclone	Cat#A6956
Rpn10 (PSMD4)	CST	Cat#12441S
Rpn11 (PSMD14)	CST	Cat#7662S
Rpt3 (PSMC4)	Enzo	Cat#BML-PW8765
PSMA7	Abcam	Cat#ab109378
PSMB5	CST	Cat#12919S
20S	Enzo	Cat#BML-PW8195
γ-tubulin	Sigma	Cat#T5326
β-actin	Genscript	Cat#A00702
Flag-beads	Sigma	Cat#A2220
Chemicals, Peptides, and Recombinant Proteins		
Lipofectamine 2000	Invitrogen	Cat# 11668019
MG-132	MCE	Cat#HY-13259
BTZ (Bortezomib)	MCE	Cat# HY-10227
Deposited Data		
Raw imaging data	This paper	https://data.mendeley.com/datasets/3d4zdm6bh7/9/files/9fe70da6-6f9e-418a-9cc8-7b04756f5d7d/source%20data%2020200509.ppt?dl=1
Raw and analyzed data	This paper	GEO: GSE140239
Experimental Models: Cell Lines		
HEK293T	ATCC	N/A
MCF-7	ATCC	HTB-22D
U2OS	ATCC	HTB 96
Oligonucleotides		
See Table S4.	N/A	N/A
Recombinant DNA		
pcDNA3-TET2-Flag	This paper	N/A
pcDNA3-mTET2-Flag	This paper	N/A
pcDNA3-Zscan4f-HA WT/3A	This paper	N/A

(*Continued on next page*)

Continued

REAGENT or RESOURCE	SOURCE	IDENTIFIER
pcDNA3-ZSCAN4-Myc WT/Mut	This paper	N/A
pMXs-Zscan4f-Flag WT/3A	This paper	N/A
pCDH-GFP-Zscan4f WT/3A		
Software and Algorithms		
GraphPad Prism 5	GraphPad Software	https://www.graphpad.com/scientific-software/prism/

RESOURCE AVAILABILITY

Lead Contact

Further information and requests for resources and reagents should be directed to and will be fulfilled by the Lead Contact, Dan Ye (yedan@fudan.edu.cn).

Materials Availability

All unique/stable reagents generated in this study are available from the Lead Contact with a completed Uniform Biological Materials Transfer Agreement.

Data and Code Availability

The CHIP sequencing data generated in this study is made available at the Gene Expression Omnibus (GEO). The accession number for the raw and processed data reported in this paper is GEO: GSE140239. We have deposited the unprocessed gel data at Mendeley data (https://data.mendeley.com/datasets/3d4zdm6bh7/9/files/9fe70da6-6f9e-418a-9cc8-7b04756f5d7d/source%20data%2020200509.ppt?dl=1).

EXPERIMENTAL MODEL AND SUBJECT DETAILS

Animals

All animal experiments were carried out in accordance with the investigator's protocol approved by the Ethics Committee of the Institutes of Biomedical Sciences, Fudan University. Mice were group-housed in individually ventilated cages and maintained under specific pathogen-free conditions. And mice were used between 10 and 14 weeks of age.

Cell lines

HEK293T and MCF-7 were obtained from the American Type Culture Collection (ATCC), and were cultured in Dulbecco's Modified Eagle's Medium (DMEM) (Invitrogen, Shanghai, China) supplemented with 5%–10% fetal bovine serum (FBS) (GIBCO), penicillin and streptomycin. U2OS cells was cultured by Roswell Park Memorial Institute (RPMI) medium (Invitrogen, Shanghai, China) supplemented with 10% fetal bovine serum (GIBCO), penicillin, and streptomycin. Furthermore, MEFs, CCL-171, feeder cells and plat-E packaging cells were cultured in MEF medium supplemented with 10% FBS.

Primary cell cultures

OG2-MEFs were derived from E13.5 embryos of C57BL/6 mice that were heterozygous for the Oct4-GFP transgenic allele. In our study, we only used MEFs within the first three passages for iPS cell generation to avoid replicative senescence. Feeder cells were generated by irradiating ICR MEFs. Moreover, iPSC cells were cultured on irradiated feeder cells in mouse ES cell medium supplemented with 10% FBS (GIBCO), L-glutamine, nonessential amino acids, 2-mercaptoethanol, sodium pyruvate, leukemia inhibitory factor (LIF) and BSA.

METHOD DETAILS

Mammalian two-hybrid assay

UAS-Luciferase reporter plasmid, CMV-Renilla control plasmid, human full-length TET2 fusing with VP16 transactivation domain, and SCAND1 fusing with Gal4 DBD were co-transfected into HEK293T cells. After transfection for 30 hr, the luciferase reporter activity was detected by a commercial kit (Promega E1910) with Turner BioSystems Luminometer Reader (Promega).

When the VP16-TET2 exists, the luciferase value is labeled as L1, and the Renilla value is labeled as R1. When the VP16-TET2 does not exist, the luciferase value is labeled as L2, and the Renilla value is labeled as R2. The relative luciferase activation is calculated as following: (L1/R1) / (L2/R2).

Transfection and immunoprecipitation

Transient transfection was performed with Lipofectamine 2000 (Invitrogen) or polyJet (SignaGen) according to the manufacturer's instruction. Cells were washed with cold phosphate buffered saline (PBS) and lysed in NP-40 buffer, containing 50 mM Tris-HCl, 300 mM NaCl, 0.3% NP-40, pH 7.4 and protease inhibitor cocktail (Roche) with rotation at 4°C for 40 min. After centrifugation at 13000 × g for 15 min at 4°C, the supernatant was incubated with appropriate antibodies for 2 hr, followed by incubation with Protein-A/G for another 1 hr at 4°C.

In vitro pull-down assay

His-tagged Zscan4f^{N155} was transformed into *Escherichia coli* BL21 and was induced with 0.2mM IPTG at 16°C. His-Zscan4f^{N155} was purified by immunoprecipitation. Flag-tagged mTet2 protein was overexpressed in HEK293T cells, and was purified by immunoprecipitation with Flag beads, followed by elution with Flag peptide (Sigma). Purified mTet2 and His-Zscan4f^{N155} were co-incubated with Flag beads at 4°C for 2 hr. The beads were collected by centrifugation at 1,800 rpm for 3 min at 4°C, and then subjected to SDS-PAGE and Coomassie blue staining.

EMSA assay

A 6-carboxy-fluorescein (FAM)-labeled double-stranded DNA (dsDNA) containing five CpG site was generated from annealing two primers (upper primer, FAM-5′-CGGGGCGCCGCCGGCCGCAGCCCG-3′; lower primer, 5′-CGGGCTGCGGCCGGCGGCG CCCCG-3′). Briefly, DNA (25 nM) and 15 mM proteins were incubated in reaction buffer containing 20 mM HEPES pH 7.4, 100 mM KCl, 1 mM DTT, 5 μm $MgCl_2$, 200 μm EDTA, 5% glycerol for 30 min at 4°C. The samples were subject to 8% PAGE and analyzed by Typhoon FLA 9500 (GE Healthcare) image scanning.

Fluorescence polarization assay

As previously described (Guo et al., 2015), FAM-labeled dsDNA (15 nM) was incubated with increasing amounts of wild-type Zscan4f or Zscan4f^{3A} mutant proteins for 30 min at 25°C in reaction buffer containing 20 mM HEPES pH 7.5, 100 mM KCl, 8% glycerol, and 0.5 mg/ml BSA. Fluorescence polarization was measured by Synergy 4 Microplate Reader (BioTek) at 25°C. Each reaction was performed in triplicate and the curves were fitted using GraphPad Prism 5.

RNA isolation and qRT-PCR analysis

Total RNA was extracted from cells by Trizol reagent (Invitrogen) and reversely transcribed with oligo-dT primers following the manufacturer's instruction. Real-time PCR was performed with gene-specific primers in the presence of SYBR Premix Ex Taq (TaKaRa) following the manufacturer's instructions. β-ACTIN was used as a housekeeping control. Primer sequences were listed in Table S4.

RNA-seq assay

The total RNA (1 μg per sample) was extracted from D4-OSKM-2ndMEFs. The RNA-seq libraries were prepared using VAHTS mRNA-seq V2 Library Prep Kit for Illumina (Vazyme) following the manufacturer's instruction, and sequenced by the Illumina sequencing platform on a 150 bp paired-end run. Sequencing reads from RNA-seq data were aligned using the spliced read aligner HISAT2, which was supplied with the Ensembl mouse genome assembly (Genome Reference Consortium GRCm38) as the reference genome. Gene expression levels were calculated by the RPKM (Reads Per Kilobase Million).

ChIP-seq assay

The DNA fragments achieved were preceded by QIAseq Ultralow Input Library Kit (QIAGEN, 180495) for library construction following the manufacturer's instruction. The workflow combines enzymatic steps and employs minimal bead-based cleanups, thereby reducing sample handling. After library construction, samples were sequenced in Novegene (Beijng, China) by Hiseq X 10 (Illumina).

Chromatin Immunoprecipitation (ChIP)-qPCR assay

ChIP-qPCR assay was performed as described previously (Lan et al., 2007). Briefly, cells were crosslinked with 1% paraformaldehyde for 10 min at room temperature and quench the cross linking reaction by adding 2.5M Glycine to a final concentration of 0.125M for 5 minutes. After sonication at 4°C, solubilized chromatin was incubated with antibodies against Flag or negative control IgG at 4°C for 3 hr, followed by incubating with Protein A-Sepharos (RepliGen). Antibody-chromatin complexes were pulled-down and washed. After crosslink reversal, the immunoprecipitated DNA was extracted with PCR Purification Kit (QIAGEN). The DNA fragments were further analyzed by qPCR using specific primers as listed in Table S4.

hMeDIP-qPCR and MeDIP-qPCR analysis

The hMeDIP and MeDIP-qPCR assays were performed as previously described (Ito et al., 2010). Briefly, 2 μg genomic DNA extracted from cells by the phenol-chloroform method was sonicated, denatured and then immunoprecipitated with antibody against 5hmC, 5mC, or negative control IgG and protein G-Sepharose (Invitrogen). After washing for three times, beads were treated with proteinase K for 4 hr. DNA was extracted with PCR Purification Kit (QIAGEN). And the DNA fragments were analyzed by qPCR using specific primers as listed in Table S4.

Somatic cell reprogramming and iPSC generation

MEFs were seeded in 6-well plates at a density of 8×10^4 cells per well in MEF medium. Twelve hours later, MEFs were infected with virus expressing indicated genes, and this day was defined as "Day 0." The culture medium was changed into mouse ES cell medium 12 hr post-infection, and refreshed daily. The number of GFP-positive colonies was counted under Olympus inverted fluorescent microscope at day 16.

ALP staining

ALP staining was performed using the Vector Red Alkaline Phosphatase Substrate Kit I (Sigma-Aldrich), in accordance with the manufacturer's protocol. Briefly, iPSCs were washed with PBS and fixed in 4% paraformaldehyde for 1 min at room temperature. After washing twice in PBS, the colonies were detected by ALP substrate for 30 min at room temperature in the darkness.

Immunofluorescence assay

Cells were fixed with 4% paraformaldehyde for 30 min at room temperature and washed with cold PBS, permeabilized with 0.3% Triton X-100 for 15 min at room temperature, and blocked with 1% BSA (Sigma) for 1 hr. And then the cells were incubated with primary antibodies at 4°C overnight, followed by staining with the respective secondary antibodies conjugated to Alexa Fluor (Invitrogen)for 1 hr at room temperature. Cell nucleus was stained with DAPI (Invitrogen).

Measurement of glucose consumption and lactate secretion

Glucose consumption and lactate secretion were measured by using the glucose assay kit (GAGO20-1KT, Sigma) and the lactate assay kit (MAK064-1KT, Sigma), respectively, according to the manufacturer's instructions.

Metabolite profiling by LC-MS/MS

Upon harvest, cells were fixed by immediate addition of 1 mL 80% (v/v) pre-cold (−80°C) methanol into culture plates. Metabolites were extracted by rotating at 4°C for 1 hr. Then the sample was centrifuged at 13,000 g for 15 min at 4°C and the supernatant was collected. Cell extracts were analyzed by ultrahigh performance liquid chromatograph (Acquity, Waters) coupled to a Q Exactive hybrid quadrupole-orbitrap mass spectrometer (Thermo Fisher).

Proteasome activity assay

D4-OSKM-2nd MEF cells were lysed with Lysis buffer (60 mM HEPES pH 7.5, 0.5 mM EDTA, 50 mM NaCl, 50 mM KCl, 10 mM MgCl2, 5% Glycerol, and 0.2% NP-40). Protein concentration was assessed with BCA Protein Assay Kit (Beyotime, P0010S). 5∼10 ng proteins were incubated with the substrate (LLVY-AMC for chymotrypsin-like activity) for 15 min at 37°C and the free AMC fluorescence was quantified using a 380/430 nm filter set in a Synergy H4 Hybrid MultiMode Microplate Reader (BioTek). All data shown represent the results obtained from triplicated independent experiments with SEM (mean ± SEM).

QUANTIFICATION AND STATISTICAL ANALYSIS

Statistical analyses were performed with a two-tailed unpaired Student's t test. All data shown represent the results obtained from triplicated independent experiments with SEM (mean ± SEM). The values of $p < 0.05$ were considered statistically significant.